Liquid Crystals
Publication details, including instructions for authors and subscription information:
http://www.tandfonline.com/loi/tlct20

Orientational order of guest molecules in aligned liquid crystal as measured by EPR and UV-vis techniques

Tatiana S. Yankova [a], Natalia A. Chumakova [a], Daria A. Pomogailo [a] & Andrey Kh. Vorobiev [a]

[a] Department of Chemistry, Lomonosov Moscow State University, Moscow, Russia

Published online: 10 May 2013.

To cite this article: Tatiana S. Yankova, Natalia A. Chumakova, Daria A. Pomogailo & Andrey Kh. Vorobiev (2013) Orientational order of guest molecules in aligned liquid crystal as measured by EPR and UV-vis techniques, Liquid Crystals, 40:8, 1135-1145, DOI: 10.1080/02678292.2013.795621

To link to this article: http://dx.doi.org/10.1080/02678292.2013.795621

Liquid Crystals, 2013
Vol. 40, No. 8, 1135–1145, http://dx.doi.org/10.1080/02678292.2013.795621

Taylor & Francis
Taylor & Francis Group

Orientational order of guest molecules in aligned liquid crystal as measured by EPR and UV–vis techniques

Tatiana S. Yankova*, Natalia A. Chumakova, Daria A. Pomogailo and Andrey Kh. Vorobiev

Department of Chemistry, Lomonosov Moscow State University, Moscow, Russia

(*Received 27 November 2012; final version received 10 April 2013*)

Orientational order of guest molecules in aligned liquid crystal 4-cyano-4′-pentylbiphenyl (5CB) is studied via optical dichroism and electron paramagnetic resonance (EPR) spectra measurements. The guest molecules used are bifunctional molecules bearing paramagnetic nitroxide group and photochromic azobenzene moiety. The bifunctional probe with rigidly bonded nitroxide and azobenzene moieties was found to align as a whole, while flexible long spacer between the moieties provides independent alignment for the nitroxide and azobenzene parts. Intermolecular interactions responsible for the alignment of azobenzene and nitroxide moieties of the probe molecules are discussed. The molecules with *cis*-configuration of azobenzene moiety are able to align in the liquid-crystalline medium, but to a lesser extent than the molecules with *trans*-configuration. Directions of orientational axes and characteristics of rotational mobility of spin probes are determined. Second, fourth and, in some cases, sixth rank order parameter values are found.

Keywords: aligned liquid crystal; guest–host effect; EPR spectra simulation; spin probes; orientation distribution function

1. Introduction

It is common knowledge that guest molecules when introduced into an aligned liquid-crystalline medium become oriented under the influence of the host matrix alignment. This phenomenon is utilised for the creation of photoactive materials – photoswitches, [1] liquid-crystal (LC) lasers [2], polymer-dispersed liquid crystals [3–5], etc. Besides, the 'guest–host' effect is widely applied for the quantitative characterisation of orientational order of liquid-crystalline media [6–22]. To choose appropriate probes and to fabricate liquid-crystalline materials with desired properties, understanding of the mechanisms of the molecular orientation processes and of the detailed characteristics of the orientation of the guest molecules in the host matrix are necessary.

Dichroic dyes are widespread dopants for liquid-crystalline media. Measurement of linear dichroism in absorption bands of the dye using UV–visible spectroscopy in polarised light is widely used for characterisation of the media alignment [6–9]. However, it is known that such measurements allow for determining of values of the second rank order parameter only [6]. More detailed information about molecular orientation can be extracted if one uses paramagnetic particles as dopants (spin probes or spin labels) [11–28]. In this case, orientational alignment and dynamics of paramagnetic molecules are revealed in electron paramagnetic resonance (EPR) spectrum line shape. Structural studies of liquid crystalline phases were carried out by G.R. Luckhurst and co-workers [11–14]. C. Zannoni et al., in particular, studied dynamics and order of spin probes in systems with 'memory effect' – hydrophobic and hydrophilic aerosol particles dispersed in nematic liquid crystals [15,16]. V. Oganesyan and co-workers [17–19] combined state-of-art molecular dynamic simulations and EPR spectroscopy for advanced study of mesophases. Method for simulation of slow-motional EPR spectra, developed by J.H. Freed and co-workers, became a widespread tool for research in dynamics and order in mesophases, polymers and biological structures [20–24]. In spite of extensive literature in this field, knowedge of the structural and dynamical characteristics of LC media is not sufficient for the understanding and prediction of properties of real materials.

Earlier, we developed a procedure which allows for determining of high-rank order parameters $<P_{jm}>$ [25–28]. The procedure is based on joint numerical simulation of EPR spectra, recorded at different orientations of the sample relative to the magnetic field of the EPR spectrometer. Essentially, determination of the high-rank order parameters is the determination of complete orientation distribution function:

$$\rho(\alpha,\beta,\gamma)=\sum_{j,m',m}\frac{2j+1}{8\pi^2}\left\langle D^{j*}_{m'm}\right\rangle D^{j}_{m'm}(\alpha,\beta,\gamma) \qquad (1)$$

where α, β, γ – Euler angles relating the sample reference frame and the molecule reference frame,

*Corresponding author. Email: ya.tatiana@gmail.com

$D^{j}_{m/m}(\alpha,\beta,\gamma)$ – Wigner's D-functions $<D^{j*}_{m'm}>$ provides a set of order parameters and angular brackets denote averaging over all molecules. Samples with axial distributions are studied most often, and in this case, the series (1) coefficients and the order parameters are related by the following expression:

$$\langle P_{jm}\rangle = \frac{\left\langle D^{j*}_{0m}\right\rangle + \left\langle D^{j*}_{0-m}\right\rangle}{2} \qquad (2)$$

The order parameter values of guest molecules in the liquid-crystalline medium are influenced by several factors, primarily by the shape of the molecules [20,29,30] and intermolecular interactions between the guest molecules and the liquid crystal molecules. One of the most interesting objects for orientational order study is azobenzene chromophore. It is known that azobenzene group undergoes *trans–cis* photoisomerisation, which leads to considerable changes in the shape of the molecules. Besides, the photoisomerisation of the azobenzene chromophores embedded in liquid-crystalline medium can be utilised to control alignment of the liquid crystal through the photo-orientation mechanism [31,32]. Thus, the purpose of the present work is to study the orientation of probe molecules bearing azobenzene moiety. To determine detailed characteristics of orientational order, we used probes combining chromophore (azobenzene group) and paramagnetic (nitroxide group) moieties in the molecule [33]. Structures of the probes used are shown in Figure 1. The probes S1 and S2 differ from each other in length and rigidity of the spacer between azobenzene and nitroxide parts.

In the present work, we compare order parameters of probe molecules S1 and S2 in aligned liquid crystal 4-*n*-pentyl-4′-cyanobiphenyl (5CB), determined through UV–visible and EPR spectroscopy, and analyse the capabilities of these methods to characterise the alignment of liquid crystal. The results obtained are compared with orientational characteristics of aligned azobenzene and 4-hydroxy-2,2,6,6-tetramethylpyperidine-1-oxyl (TEMPOL), which can be considered as parts of the bifunctional probes S1 and S2.

2. Experimental part

2.1 Sample preparation

Alignment of LC samples was produced by either of the two methods: (1) by the action of magnetic field of EPR spectrometer on the liquid crystal followed by rapid cooling of the sample with liquid nitrogen (77 K) or (2) by embedding the LC in stretched porous polyethylene film where LC is oriented by the action of pores surface. The samples will be referred below as type I and type II samples, correspondingly.

Maximum orientational alignment of the liquid crystal is achieved in the samples of type I, but in this case, EPR spectra at different orientations of the sample relative to magnetic field of the spectrometer were recorded only for frozen sample (at 77 K) to avoid reorientation of liquid-crystalline director by the magnetic field. EPR spectra of the samples of type II were registered at 77 K and at 295 K, since the action of pores surface is stronger than the action of the magnetic field of EPR spectrometer and reorientation of the liquid-crystalline director in this case does not occur.

Liquid crystal 5CB from Merck (Darmstadt, Germany) was used without further purification. It exhibits nematic phase within temperature range 293–320 K. Stretched porous polyethylene films were prepared according to procedure described in Ref. [34] and were kindly granted to us by Prof. G.K. Elyashevitch (Institute of Macromolecular Compounds, RAS, Russia). The films have thickness of 0.05 mm and oriented elongated pores (average diameter 200 nm) capable of aligning embedded liquid crystals [35,36].

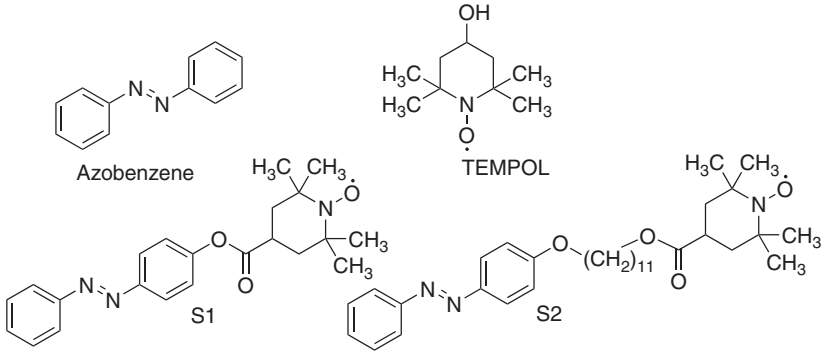

Figure 1. Structures of probes used.

Spin probe TEMPOL from Sigma Aldrich (St. Louis, MO, USA) was used without further purification. Probes S1 and S2 were synthesised according to the procedure described in Ref. [33] and were kindly granted to us by Prof. S. Nakatsuji (University of Hyogo, Japan).

The probes were introduced into the liquid crystal 5CB at concentration $\sim 10^{-3}$ M. To prepare aligned sample of type I, the liquid crystal containing admixture of the probe was placed into quartz ampoule for EPR measurements. The ampoule, in turn, was placed in quartz Dewar vessel with a cold finger entering the resonator of the spectrometer. The sample was kept in the magnetic field of the spectrometer (0.5 T) for 5 minutes (at 295 K). After that, the sample was cooled down to 77 K by pouring of liquid nitrogen in the Dewar vessel in the magnetic field of the EPR spectrometer.

To prepare the sample of type II liquid crystal with the probe, admixture was applied on the porous polyethylene film surface. The mixture was readily soaked into the film due to the surface action. The rest of the mixture was thoroughly removed from the film surface. To increase volume of the sample for EPR spectroscopy, 10 layers of the film were put together to form a 'sandwich' with a fixed pores direction. The dimensions of sample II were $15 \times 3 \times 0.5$ mm^3.

2.2 *Photochemical* **trans–cis** *isomerisation of the probes*

To carry out photochemical *trans–cis* isomerisation of probes S1, S2 and azobenzene, the samples of type I and II were irradiated at 295 K with light of mercury lamp at a wavelength of 365 nm (using standard light filter). Completeness of the reaction was checked by the use of UV–visible spectroscopy.

2.3 *Registration of EPR and UV–visible spectra*

EPR spectra were recorded with X-band spectrometer Varian-E3 (Varian Inc., Palo Alto, CA, USA). EPR spectra at 77 K were registered using a quartz Dewar filled with liquid nitrogen. EPR spectra were registered at different angles between magnetic field vector and the sample anisotropy axis with a 10° step. The sample was turned around the axis perpendicular both to the magnetic field and to the sample anisotropy axis. Turn angles were set with accuracy of $\pm 0.2°$ using a goniometer. The set of spectra obtained in the course of such a procedure is referred to as angular dependence of EPR spectrum. All experimental spectra were normalised so that the double integral of each spectrum was equal to unity.

UV−visible spectra in polarised light were registered using spectrophotometer SPECORD M40 with a polarising Glan prism. For registration of UV–visible spectra, only one layer of stretched porous polyethylene film filled with doped liquid crystal was used.

Optical dichroism values were calculated using the following expression:

$$d = \frac{A_{\text{par}} - A_{\text{per}}}{A_{\text{par}} + 2A_{\text{per}}} \tag{3}$$

where A_{par} and A_{per} are values of absorbance at parallel and perpendicular polarisation directions of a probe beam relative to the sample director, respectively.

Anisotropic light scattering of the samples was taken into account by extraction of different baselines from the UV–visible spectra, registered at parallel and perpendicular polarisation directions of a probe beam relative to the sample director. Optical dichroism values were measured for absorption band, corresponding to n–π^* transition, with absorption maximum at $\lambda = 440$ nm. Optical dichroism values were determined as averages in the wavelength range 430–450 nm.

2.4 *Numerical simulation of EPR spectra registered at 77 K*

Numerical simulation of EPR spectra registered at 77 K was carried out according to the procedure described in detail in Refs. [27,28]. The numerical simulation of EPR spectra includes minimisation of deviations of calculated spectra from experimental ones (discrepancy). The discrepancy is taken as follows:

$$D = \frac{1}{2}\sum_i \frac{r_i^2}{n} \tag{4}$$

where r_{i} is the difference of intensities between calculated and experimental spectra, and n is number of points in the spectrum.

The discrepancy was minimised using an adaptive nonlinear least-squares algorithm described in Ref. [37]. The calculation of EPR spectra was performed in a weak external field approximation up to the second order of the perturbation theory. Principal axes of hyperfine interaction tensor were assumed to coincide with g-tensor principal axes. Individual line shape was described by convolution of Gaussian and Lorentzian functions.

Gaussian and Lorentzian linewidths were second-rank tensors, which were used to take into account the anisotropy of linewidths. Linewidth axes were assumed to coincide with g-tensor principal axes.

Magnetic parameters (components of g-tensor and tensor of hyperfine interaction) of the spin probe were

Table 1. Magnetic resonance parameters of the spin probes used.

	TEMPOL	S1	S2
g_x*	2.0092	2.0093	2.0092
g_y	2.0062	2.0059	2.0061
g_z	2.0020	2.0020	2.0019
A_x, G	7.0 ± 0.5	7.1 ± 0.4	7.45 ± 0.5
A_y, G	5.6 ± 1.0	5.9 ± 0.4	6.03 ± 0.5
A_z, G	35.1 ± 0.1	33.91 ± 0.1	34.56 ± 0.1

Note: *Errors of determination of g-tensor components are ±0.0002.

determined by simulation of EPR spectra of isotropic sample at 77 K at rigid limit conditions. The parameters for spin probes TEMPOL, S1 and S2 are given in Table 1. Within the accuracy of the method, g-tensor values are similar for all the three spin probes.

The determined magnetic parameters have been used for the numerical simulation of the angular dependencies of EPR spectrum. Characteristics of orientation distribution function were determined through joint numerical simulation of 10–15 EPR spectra, recorded at different angles between the sample symmetry axis and the EPR spectrometer magnetic field direction. As a result of such simulation, orientation distribution function of orientational axis of the spin probe can be determined [27,28]. Orientation distribution function was determined using assumption of axial interaction between the probe molecule and the aligned medium. In this case, the orientation distribution function (1) depends on the angle δ between orientational axis and the liquid crystal director and can be expressed as follows [11,38,39]:

$$\rho(\delta) = \sum_{j=0}^{\infty} \frac{2j+1}{2} \left\langle P_{j0} \right\rangle P_{j0}(\cos\delta) \qquad (5)$$

where $P_{j0}(\cos\delta)$ represent Legendre polynomials, and $<P_{j0}>$ represent order parameters of orientational axis.

The parameters of the minimisation procedure are order parameters $<P_j>$ and angles (θ, φ), which relate orientational axis direction and g-tensor principal axes. Angle θ is the angle between axis g_z and the orientational axis, angle φ is angle between projection of the orientational axis on the $g_x g_y$ plane and g_x axis.

The series (5), restricted up to certain $j_{\max}$ was used in the procedure of simulation. To choose necessary truncation $j_{\max}$ of a series (5), the following procedure was used. Numerical simulation of experimental EPR spectra was carried out with truncation of a series (5) up to term j (expansion rank is j), then simulation was repeated with expansion rank $j + 2$. If the value of difference between optimal minimisation functions $D_j - D_{j+2}$ is substantially less than value of experimental noise, expansion of rank j was considered as sufficient to fit the EPR spectra. Otherwise, terms of rank $j + 2$ were added in a series (5). We estimated the experimental noise value as the mean-squared intensity of EPR spectrum in the region of 'tails' of the spectrum, where paramagnetic signal is absent (as it was made in Ref. [40]), and error of turn angle setting was also taken into account.

One can see from Table 2 that the sixth order parameters are significant in three cases: *trans*-S1, *trans*-S2 and *cis*-S2 probes in 5CB, aligned by magnetic field. For others cases $j_{\max} = 4$ in series (3) is sufficient. Typical results of the simulation are shown in Figure 2 (a).

Orientation distribution function (5) is a distribution of orientational axis of the probe molecule in the sample frame (SF), the liquid crystal director frame. To visualise the extent of order and direction of principal orientational axis with respect to the magnetic tensor of the probe simultaneously, we transformed the distribution (5) to distribution of the sample director in principal axes of spin probe g-tensor (magnetic frame, gF). The transformation of the coefficients is implemented using the following formula:

$$\left\langle D^j_{m\prime m} \right\rangle_{\mathrm{gF}} = \sum_{k=-j}^{j} \left\langle D^j_{m'k} \right\rangle_{\mathrm{MOF}} D^j_{mk}(\varphi, \theta, 0) \qquad (6)$$

Orientation distribution functions in this work are given in magnetic principle axes frame; they are plotted in cartesian frame using expansion coefficients $\left\langle D^j_{m'm} \right\rangle_{gF}$.

Table 2. Comparison of discrepancy decrease in calculation with $j_{\max} = 4$ and 6 and the 'noise level'.

Probe	TEMPOL	*trans*-S1	*cis*-S1	*trans*-S1	*cis*-S1	*trans*-S2	*cis*-S2	*trans*-S2	*cis*-S2
Alignment type	Magnetic field			PE pores		Magnetic field		PE pores	
$D_4 - D_6$*	2.6×10^{-12}	9×10^{-11}	9×10^{-12}	2×10^{-11}	4×10^{-13}	3.4×10^{-11}	3.4×10^{-11}	2×10^{-12}	1×10^{-12}
$\frac{D_4 - D_6}{D_4}$, %	0.8	3	0.6	2	1	1	1	0.1	0.2
Noise level	3.0×10^{-10}	8.5×10^{-11}	1.3×10^{-10}	7.7×10^{-10}	1.7×10^{-11}	2.4×10^{-12}	1.9×10^{-12}	1.1×10^{-11}	7.5×10^{-11}

Note: *Squared roots of the presented D_j values are the variance for one point of spectrum with unit area.

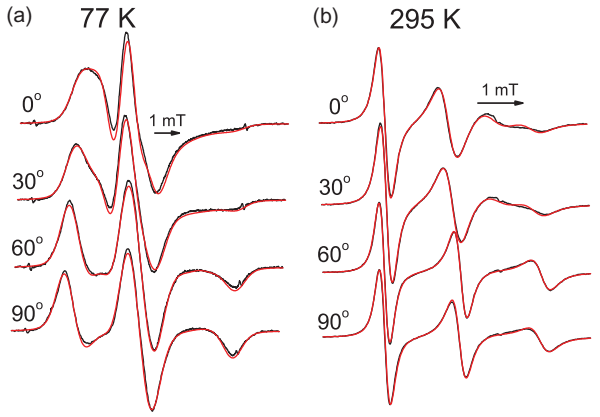

Figure 2. (colour online) Experimental spectra (black line) and simulated spectra (red line) of probe *trans*-S1 in 5CB, (a) the sample is aligned by magnetic field, $T = 77$ K and (b) the sample is aligned by pores of stretched porous polyethylene film, $T = 295$ K.

2.5 *Numerical simulation of EPR spectra, registered at 295 K*

Numerical simulation of EPR spectra, registered at 295 K was carried out according to the method described in Refs. [23,24,40]. The software for calculation of slow-motional magnetic resonance spectra, developed by J.H. Freed and coauthors [24], was employed. We modified this software to simulate a set of EPR spectra (angular dependence) jointly.

Within this approach, orientational order of spin probe molecules is induced by Brownian rotational diffusion in orienting potential $U(\Omega)$. Then according to Boltzmann equilibrium law, the orientation distribution function is as follows:

$$\rho(\Omega) = \frac{e^{-U(\Omega)/k_bT}}{\int_\Omega e^{-U(\Omega)/k_bT}\mathrm{d}\Omega} \tag{7}$$

Here Ω are Euler angles connecting rotational diffusion tensor and director reference frame (sample frame, SF). In case of cylindrical symmetry of director, $\Omega = (0, \beta, \gamma)$. The orienting potential is expanded in a series of spherical Wigner's D-functions:

$$\begin{aligned}\frac{U(\beta,\gamma)}{k_bT} &= -\sum_j c_{j0}D^j_{00}(\beta,\gamma) \\ &\quad -\sum_{j,m} c_{jm}\left[D^j_{0m}(\beta,\gamma) + D^j_{0-m}(\beta,\gamma)\right]\end{aligned} \tag{8}$$

Sought parameters of this model are rotational diffusion coefficients (R_x, R_y, R_z) of the probe, orienting potential expansion coefficients (c_{jm}) and Euler angles

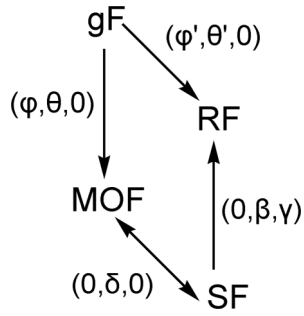

Figure 3. Reference frames used: SF-sample frame, MOF-molecular orientational frame, RF-molecular rotational frame, gF-frame of g-tensor principal axes.

(θ',φ') relating rotational diffusion tensor and reference frame of g-tensor principal axes of a paramagnetic molecule.

All spin probes in this work were found to have axial symmetry of rotational diffusion tensor ($R_x = R_y$). R_z coefficient corresponds to the fastest rotational axis. Thus, there are two angles (θ',φ') relating the fastest rotational axis and magnetic frame (g-tensor principal axes frame).

Order parameters are calculated according to the following expression:

$$\langle P_{jm}\rangle = \frac{\int e^{-U(\beta,\gamma)/k_bT}(D^j_{0m} + D^j_{0-m})\sin\beta d\beta d\gamma}{2\int e^{-U(\beta,\gamma)/k_bT}\sin\beta d\beta d\gamma} \tag{9}$$

Typical results of the simulation of EPR spectra recorded at 295 K are shown in Figure 2 (b).

Orientation distribution function, which is given by coefficients $<P_{jm}>$ in (9) is then transformed to distribution function of the sample director in g-tensor frame via rotation. Relations between all the reference frames are shown in Figure 3.

3. Results

3.1 *Orientation distribution of spin probes in 5CB, aligned by magnetic field*

In Figure 4, EPR spectrum angular dependencies of probes TEMPOL, S1 and S2 in 5CB, aligned by magnetic field of the EPR spectrometer, are shown. One can see that the angular dependence of *trans*-S1 is much stronger than angular dependence of *cis*-S1, while angular dependencies of probes TEMPOL, *trans*-S2 and *cis*-S2 look very similar. Parameters of orientation distribution function (Table 3) change significantly from *trans*-S1 to *cis*-S1: order parameters values decrease, angles (θ,φ), determining direction of orientational axis of the probe change. Thus, molecules of *trans*-S1 and *cis*-S1 align in the liquid

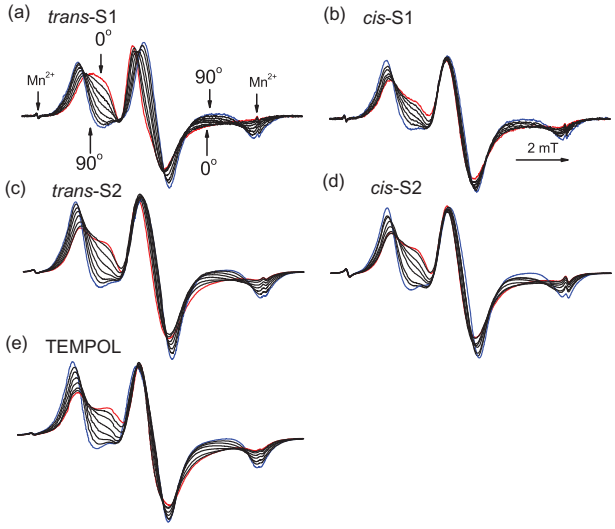

Figure 4. (colour online) Angular dependencies of EPR spectra of spin probes S1 and S2 in 5CB, aligned by magnetic field, recorded at 77 K (a) *trans*-S1; (b) *cis*-S1; (c) *trans*-S2; (d) *cis*-S2 and (e) TEMPOL.

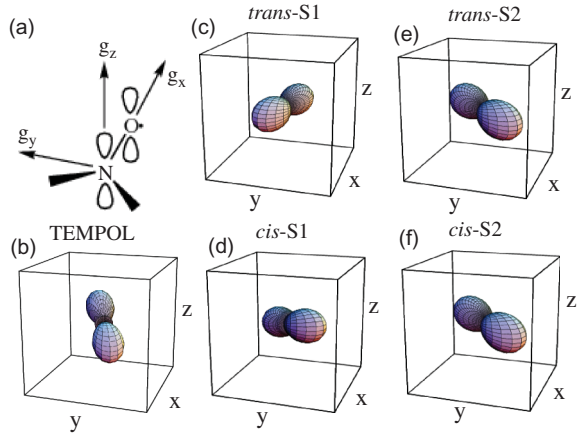

Figure 5. (colour online) (a) Nitroxide principal g-tensor axes; ODFs of different spin probes in 5CB, aligned by magnetic field, 77 K. The functions are plotted in principal axes of g-tensor reference frame; (b) TEMPOL; (c) *trans*-S1; (d) *cis*-S1; (e) *trans*-S2 and (f) *cis*-S2.

crystal in different ways. On the contrary, parameters of orientation distributions for *trans*-S2 and *cis*-S2 are almost coincident.

Orientation distribution functions of spin probes S1, S2 and TEMPOL are shown in Figure 5.

3.2 Orientation distribution of spin probes in 5CB, aligned by pores of stretched porous polyethylene film

Orientation distribution of probes S1 and S2 in samples of type II, cooled down to 77 K was found to be qualitatively similar to distributions of the probes in samples of type I. The difference consists in lower values of order parameters in case of samples of type II (compare values in Tables 3 and 4). It is seen from Tables 3 and 4, that angle θ in case of probe *cis*-S1 is 101.7° ± 0.9° for sample of type I and 89.9° ± 1.0° for sample of type II. We suppose that this difference lies within errors of determination of the parameter and the values of errors given here are underestimated.

The angular dependencies of EPR spectra of probes S1 and S2 in *trans* and *cis* configurations in samples of type II, registered at 295 K, are shown in Figure 6. Similarly to EPR spectra recorded at 77 K, in this case angular dependencies of EPR spectra of probes *trans*-S1 and *cis*-S1 are significantly different, while they are quite similar for *trans*-S2 and *cis*-S2 probes. Parameters, determined through simulation of EPR spectra for samples of type II at 295 K are shown in Table 4. They include orienting potential coefficients (Equation 8), rotational diffusion coefficients R_x, R_y, R_z and angles (θ', φ').

One can see corresponding orientation distribution functions in Figure 7. As it is seen from Table 4, orientation distributions of probes *trans*-S2 and *cis*-S2 in the samples of type II are almost the same both at 77 K and 295 K. Thus, the configuration of the azobenzene moiety of the molecule S2 does not influence orientational order and rotational mobility of the nitroxide moiety.

In case of probe S1, there is considerable difference between distributions of *trans*- and *cis*-probes at both temperatures. It should be noted that characteristics of

Table 3. Orientation distribution function parameters of spin probes TEMPOL, *trans*-S1, *cis*-S1, *trans*-S2, *cis*-S2 in 5CB, aligned by magnetic field*.

	TEMPOL	*trans*-S1	*cis*-S1	*trans*-S2	*cis*-S2
$<P_{20}>$	0.432 ± 0.006	0.470 ± 0.003	0.329 ± 0.007	0.373 ± 0.002	0.371 ± 0.002
$<P_{40}>$	0.277 ± 0.017	0.102 ± 0.003	0.077 ± 0.007	0.089 ± 0.003	0.074 ± 0.002
$<P_{60}>$	–	0.032 ± 0.003	0.041 ± 0.015	0.022 ± 0.003	0.021 ± 0.003
θ(°)	75.5 ± 0.3	91.5 ± 1.8	101.7 ± 0.9	89.4 ± 2.6	89.4 ± 2.6
φ(°)	65.1 ± 0.4	7.2 ± 1.2	49.5 ± 0.3	46.2 ± 0.3	46.5 ± 0.32

Notes: *Here and in further tables, the values of errors of the parameters are estimated according to the procedure described in Ref. [40]. The values of errors seem to be underestimated.

Table 4. Parameters of simulation of angular dependencies of EPR spectra (77 K and 295 K) of probes *trans*-S1, *cis*-S1, *trans*-S2, *cis*-S2 in 5CB aligned in stretched porous PE film.

	trans-S1	*cis*-S1	*trans*-S2	*cis*-S2
77 K	$<P_{20}> = 0.375 \pm 0.001$ $<P_{40}> = 0.055 \pm 0.001$ $<P_{60}> = 0.017 \pm 0.002$ $\theta = 89.2° \pm 0.6°$ $\varphi = 9.4° \pm 0.8°$	$<P_{20}> = 0.218 \pm 0.001$ $<P_{40}> = 0.021 \pm 0.001$ $<P_{60}> = 0.0 \pm 0.0014$ $\theta = 89.9° \pm 1.0°$ $\varphi = 47.7° \pm 0.2°$	$<P_{20}> = 0.299 \pm 0.014$ $<P_{40}> = 0.040 \pm 0.007$ $<P_{60}> = 0.007 \pm 0.004$ $\theta = 83.9° \pm 4.0°$ $\varphi = 44.6° \pm 0.3°$	$<P_{20}> = 0.287 \pm 0.03$ $<P_{40}> = 0.035 \pm 0.010$ $<P_{60}> = 0.009 \pm 0.009$ $\theta = 83.9° \pm 8.4°$ $\varphi = 52.5° \pm 0.6°$
295 K	$c_{20} = 1.239 \pm 0.007$ $c_{22} = -0.080 \pm 0.002$ $\theta' = 106.4° \pm 0.2°$ $\varphi' = 10.2° \pm 0.3°$ $R_x = R_y = (1.22 \pm 0.02) \times 10^7 s^{-1}$ $R_z = (6.47 \pm 0.07) \times 10^8\ s^{-1}$	$c_{20} = 0.231 \pm 0.002$ $c_{22} = -0.121 \pm 0.001$ $c_{40} = 0.22 \pm 0.01$ $c_{42} = 0.17 \pm 0.01$ $c_{44} = 0.26 \pm 0.01$ $\theta' = 90.0° \pm 1.2°$ $\varphi' = 5.4° \pm 0.08°$ $R_x = R_y = (3.95 \pm 0.02) \times 10^7\ s^{-1}$ $R_z = (5.50 \pm 0.1) \times 10^8\ s^{-1}$	$c_{20} = 0.486$ $\theta' = 91.4°$ $\varphi' = 41.3°$ $R_x = R_y = 7.9 \times 10^7\ s^{-1}$ $R_z = 4.9 \times 10^8\ s^{-1}$	$c_{20} = 0.474$ $\theta' = 91.0°$ $\varphi' = 39.6°$ $R_x = R_y = 7.3 \times 10^7\ s^{-1}$ $R_z = 6 \times 10^8\ s^{-1}$
Order parameters, calculated from the orienting potential parameters c_{jm}, according to formula (9)				
	$<P_{20}> = 0.275$ $<P_{22}> = -0.010$ $<P_{40}> = 0.050$ $<P_{42}> = -0.0029$ $<P_{60}> = 0.0065$	$< P_{20} > = 0.046$ $< P_{22} > = -0.026$ $< P_{40} > = 0.030$ $< P_{42} > = 0.020$ $< P_{44} > = 0.028$ $< P_{60} > = 0.00005$	$< P_{20} > = 0.103$ $< P_{22} > = 0$ $< P_{40} > = 0.0073$ $< P_{42} > = 0$ $< P_{60} > = 0.00037$	$< P_{20} > = 0.100$ $< P_{22} > = 0$ $< P_{40} > = 0.0069$ $< P_{42} > = 0$ $< P_{60} > = 0.00034$

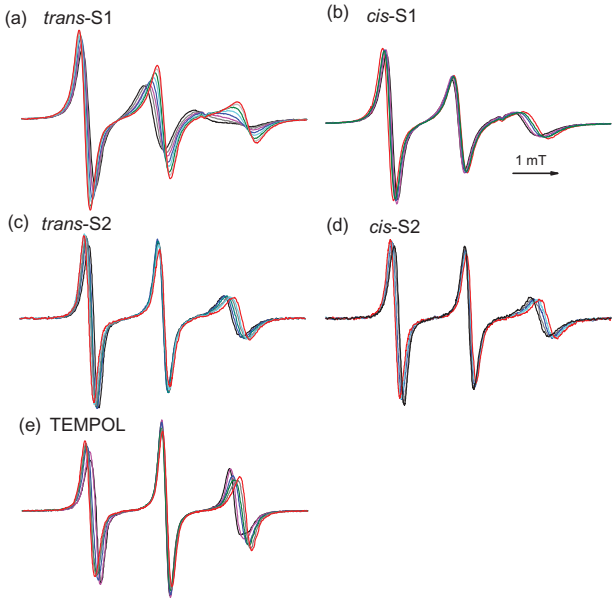

Figure 6. (colour online) Angular dependencies of EPR spectra of spin probes in 5CB aligned in stretched porous polyethylene film, recorded at 295 K: (a) *trans*-S1; (b) *cis*-S1; (c) *trans*-S2; (d) *cis*-S2 and (e) TEMPOL.

orientational order for the samples at 295 K (the last row of Table 4) were calculated from the found coefficients of orienting potential using Equations (7)–(9).

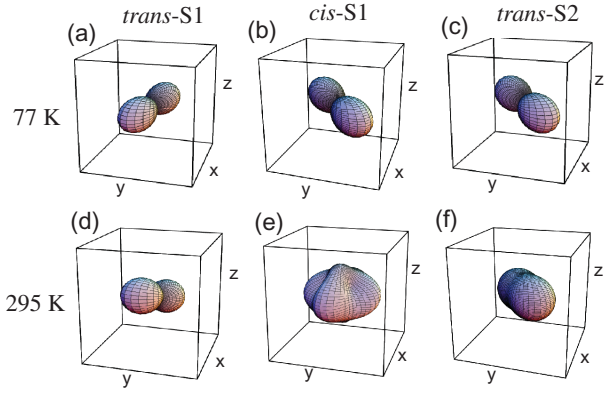

Figure 7. (colour online) Orientation distribution function of probes *trans*-S1, *cis*-S1, *trans*-S2 in 5CB, aligned in stretched porous polyethylene film, at 77 K (a, b, c) and at 295 K (d, e, f).

From Table 4 and Figure 7 (a,d), one can see that orientation distributions of *trans*-S1 probe at 77 K and at 295 K are similar qualitatively whereas they differ quantitatively.

In case of probe *cis*-S1, the orientation distribution at 295 K looks very strange. Distribution does not show a preferential orientational axis values of order parameters which are too low and, as it is shown below, contradict results of optical measurements. This result can be accounted for by noncoincidence

of orientational axis and the fast rotation axis in the paramagnetic molecule, while the method based on Equations (7)–(9) intrinsically implies coincidence of these axes.

In case of elongated molecule of *trans*-S1, the molecular orientation axis and axis of fast rotation almost coincide. Comparison of the values of angles θ and θ' for *trans*-S1 gives the angle between these axes to be about 17°. This slight difference between the orientational axis and the fast rotation axis may be the cause for the fact that higher values of order parameters are determined at 77 K than the values determined at 295 K. Probably, constrained mobility of the probe at 77 K is also responsible for higher values of order parameters at 77 K.

Cis-S1, on the contrary, is a bent-shaped molecule and the angle between orientational axis and fast rotation axis was found to be about 42°. Orientational characteristics of *cis*-S1 extracted from EPR spectra recorded at 77 K and at 295 K differ significantly. To compare the order parameters determined using EPR and UV–visible spectroscopy, we will use orientational characteristics values determined for EPR spectra recorded at 77 K, using the method based on formula (3).

Parameters of rotational mobility of probes *trans*-S1, *trans*-S2 and *cis*-S2 were also estimated through numerical simulation of EPR spectra recorded at 295 K. It is obvious that in case of nonrigid spin probe molecule (like S2), several types of molecular and intermolecular rotation may occur. Using EPR spectroscopy, we determine principal values of rotational diffusion tensor averaged over all possible molecular rotations. It was found that rotational diffusion tensor of probe S1 is much more anisotropic than one of S2. Anisotropy parameter of rotational diffusion $Rr = R_z/R_x$ for *trans*-S1 was found to be 53.0, but for *trans*-S2 and *cis*-S2 it was only 6.2.

3.3 *Linear dichroism of type II samples at 295 K*

UV–visible spectra of samples of 5CB aligned in stretched porous PE film probed with azobenzene in *trans*- and *cis*-configurations are shown in Figure 8. Spectra for the samples probed with S1 and S2 are very similar to these. The calculated values of dichroism for each sample are given in Table 5. One can see that dichroism value for *trans*-configuration is two times higher than for *cis*-configuration of the probes. Besides, the corresponding values are close for all the probes. Obtained values of dichroism and values of second order parameter determined through analysis of EPR spectra will be compared in the next section.

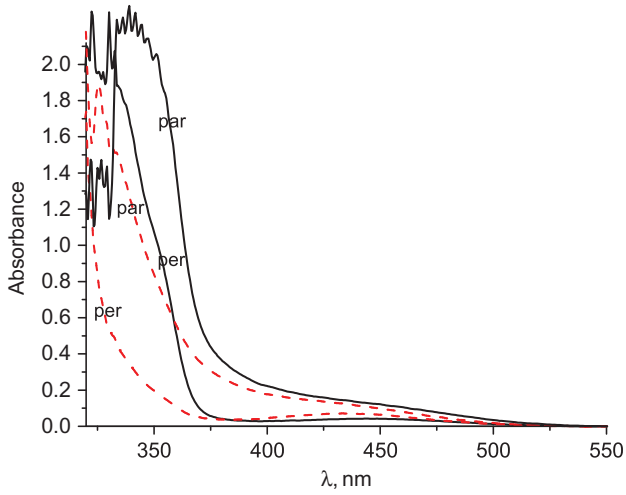

Figure 8. (colour online) UV–visible spectra of sample of azobenzene doped 5CB aligned in stretched porous polyethylene film before photoisomerisation (solid lines) and after irradiation with 365 nm light (dashed lines). The spectra were recorded at parallel and perpendicular polarisations of irradiating and probing beams.

Table 5. Linear dichroism of 5CB aligned in stretched porous PE film (averaged value within the range of $\lambda = 430$–450 nm).

Probe	*trans*	*cis*
S1	0.39 ± 0.02	0.19 ± 0.02
S2	0.36 ± 0.02	0.14 ± 0.02
Azobenzene	0.43 ± 0.02	0.18 ± 0.02

4. Discussion

Linear dichroism values for samples probed with S1, S2 and azobenzene coincide within experimental error (Table 5). Thus, orientation of azobenzene chromophore does not depend on the substituent structure. Meanwhile, order parameters found using analysis of EPR spectra turned out to be different for S1 and S2 probes. It may be supposed that the orientation of azobenzene moiety is caused by interaction of the azobenzene aromatic system with 5CB aromatic system, as is sketched in Figure 9 (a). Significant decrease of dichroism value as a result of *trans–cis* isomerisation of azobenzene moiety occurs due to worse alignment of the bent *cis*-molecules in the ordered liquid crystalline matrix in comparison with rod-like molecules of the probe in *trans*-configuration.

Experimentally determined value of dichroism d is related to the true order parameter of the chromophore molecule $<P_2>^{UV}$ by the following relation:

$$\langle P_2 \rangle^{UV} = \frac{d}{P_2(\cos \chi)} \qquad (10)$$

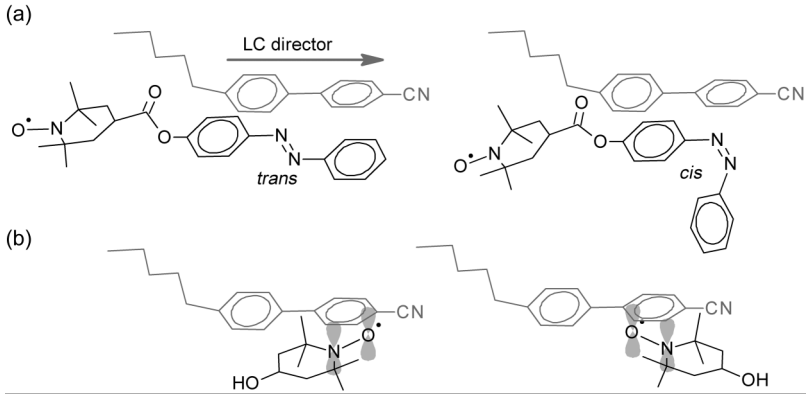

Figure 9. (a) Scheme of orientation of probes *trans*-S1 and *cis*-S1 with respect to 5CB molecules and (b) scheme of TEMPOL molecules orientation in aligned 5CB.

where χ is the angle between orientational axis and the direction of the dipole transition moment of the dye.

Thus, the value of dichroism depends on the direction of molecular dipole transition moment with respect to the orientational axis of the molecule. In case of probe S1, experimentally determined values of dichroism coincide with $<P_{20}>$ order parameters of orientational axis of paramagnetic moiety within experimental error range (Tables 4 and 5). One can conclude that the direction of the dipole transition moment coincides with the orientational axis for *trans*- and *cis*-configurations of spin probe S1. Indeed, according to quantum mechanical calculations, the dipole transition vector of n–π^* transition of *trans*-azobenzene lies in *xy*-plane, approximately, along the long axis of the molecule and forms angle ~50° with *x*-axis, as shown in Figure 10 [41,42]. The orientational axis determined via EPR spectral analysis is directed in the same way.

Azobenzene moiety in *cis*-configuration has two possible conformers, which differ in angle between planes of azobenzene rings. Dipole n–π^* transition direction for these conformers has also two possible directions in *xy*-plane [41–43] (see Figure 10).

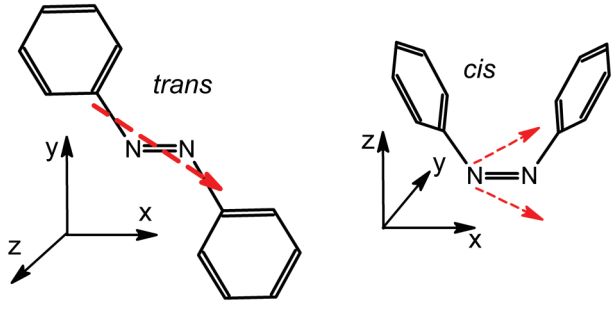

Figure 10. (colour online) *Trans*- and *cis*-azobenzene molecules. Dashed arrows are dipole transition moment directions. [41,42]

Conversion between these conformers is a high-frequency transition. Thus dipole transition direction 'fluctuates' rapidly between two directions and the averaged dipole transition moment is approximately along azobenzene N–N bond. According to the results of our experiments, this direction is given by angles θ and φ in g-tensor reference frame (shown in Tables 3 and 4). Verification of this sentence can be realised using precise quantum calculations, taking into account all the possible conformations of the molecule.

In contrast with probe S1, configuration of azobenzene moiety of probe S2 does not influence significantly on the orientation distribution of nitroxide moiety (Tables 3 and 4). The orientation distribution functions of *trans*- and *cis*-S2 determined through analysis of EPR spectra are similar to the distribution of TEMPOL (Figure 5), but direction of orientational axis slightly deviates. Thus, nitroxide and azobenzene fragments in S2 molecule align in the liquid crystalline media independently due to long flexible spacer $C_{11}H_{22}$ separating these molecular fragments. The orientation distribution of the nitroxide fragment reflects relative orientation of the nitroxide fragment and 5CB molecules. Probably, the orientational order in this case is determined by the interaction of π-orbitals of N–O bond of the nitroxide with aromatic π-system of one of the rings of 5CB molecule, as is sketched in Figure 9 (b).

5. Conclusion

Combined application of EPR and UV–visible spectroscopy techniques allowed determining the directions of molecular orientation axes of bifunctional probe molecules bearing azobenzene and nitroxide moieties aligned in nematic liquid crystalline medium. It was shown that the factor which determines the

orientation of azobenzene fragment of the molecule is the interaction of aromatic systems of azobenzene group with aromatic rings of 5CB. Bifunctional probe with a short and rigid spacer between azobenzene and nitroxide fragments aligns as a whole, while flexible long spacer between the moieties provides independent alignment for the molecular fragments. The probe molecules with short spacer in *cis*-configuration align to a lesser extent than the molecules in *trans*-configuration. Directions of orientational axes, characteristics of orientation distribution functions and rotational mobility of the probes were determined. Using EPR spectroscopy, one can extract high rank order parameters, i.e. fine features of orientational order can be obtained. In the present work, values of forth and in some cases sixth rank order parameters were estimated.

Acknowledgements

The authors are grateful to Prof. S. Nakatsuji (University of Hyogo, Japan) for the provision of bifunctional probes and to Prof. G.K. Elyashevitch (Institute of Macromolecular Compounds, RAS, Russia) for the provision of stretched porous polyethylene.

The work was supported by Russian Foundation for Basic Research, grant No. 12-03-31114.

References

[1] Feringa BL, van Delden RA, Koumura N, Geertsema EM. Chiroptical molecular switches. Chem Rev. 2012;100:1789–1816.
[2] Coles H, Morris S. Liquid-crystal lasers. Nat Photonics. 2010;4:676–685.
[3] Liu YJ, Zheng YB, Shi J, Huang H, Walker TR, Huang TJ. Optically switchable gratings based on azo-dye-doped, polymer-dispersed liquid crystals. Opt Lett. 2009;34:2351–2353.
[4] Fuh AY-G, Tsai M-S, Huang L-J, Liu T-C. Optically switchable gratings based on films doped with a guest-host dye. Appl Phys Lett. 1999;74:2572–2574.
[5] Simoni F, Cipparrone G, Mazzulla A, Pagliusi P. Polymer dispersed liquid crystals: effects of photorefractivity and local heating on holoraphic recording. Chem Phys. 1999;245:429–436.
[6] Michl J, Thulstrup EW. Spectroscopy with polarized light: solute alignment by photoselection in liquid crystals, polymers and membranes. New York (NY): VCH Publishers; 1986.
[7] Bauman D, Moryson H, Wolarz E. Study of nematic order in guest-host mixtures by polarized optical spectroscopy. J Mol Struct. 1994;325:169–175.
[8] Bauman D, Chrzumnicka E, Wolarz E. Molecular orientation in liquid crystalline side chain polymers doped with dichroic dye as studied by optical spectroscopy methods. Mol Cryst Liq Cryst. 2000;352:67–76.
[9] Wolarz E, Chrzumnicka E, Fischer T, Stumpe J. Orientational properties of 1,3,4-oxadiazoles in liquid-crystalline materials determined by electronic absorption and fluorescence measurements. Dyes Pigments. 2007;75:753–760.
[10] Chapoy LL, DuPre DB. Polarized fluorescence measurements of orientational order in a uniaxial liquid crystal. J Chem Phys. 1979;70:2550–2553.
[11] Luckhurst G, Yeates RN. Orientational order of a spin probe dissolved in nematic liquid crystals. J Chem Soc Faraday Trans 2. 1976;72:996–1009.
[12] Le Masurier PJ, Luckhurst GR. Structural studies of the intercalated smectic C phases formed by the non-symmetric α-(4-cyanobiphenyl-4′-yloxy)-ω-(4-alkylanilinebenzylidene-4′-oxy) alkane dimers using EPR spectroscopy. J Chem Soc Faraday Trans. 1998;94:1593–1601.
[13] Luckhurst GR. On the creation of director disorder in nematic liquid crystals. Thin Solid Films. 2006;509:36–48.
[14] Imrie CT, Ionescu D, Luckhurst GR. Molecular organization of the polymer backbone in a side group liquid crystal polymer. An ESR investigation. Macromolecules. 1997;30:4597–4600.
[15] Arcioni A, Bacchiocchi C, Vecchi I, Venditti G, Zannoni C. A comparison of the effects of dispersed hydrophobic or hydrophilic aerosil nanoparticles on the order and dynamics of the 5CB liquid crystal. Chem Phys Lett. 2004;396:433–441.
[16] Arcioni A, Bacchiocchi C, Vecchi I, Venditti G, Zannoni C. Electron spin resonance studies of order and dynamics in a nematic liquid crystal containing a dispersed hydrophobic aerosil. J Phys Chem B. 2002;106:9245–9251.
[17] Oganesyan VS, Kuprusevicius E, Gopee H, Cammidge AN. Electron paramagnetic resonance spectra simulation directly from molecular dynamics trajectories of a liquid crystal with a doped paramagnetic spin probe. Phys Rev Lett. 2009;102:013005-1–013005-4.
[18] Kuprusevicius E, Edge R, Gopee H, Cammidge AN, McInnes EJL, Wilson MR, Oganesyan VS. Prediction of EPR spectra of liquid crystals with doped spin probes from fully atomistic molecular dynamics simulations: exploring molecular order and dynamics at the phase transition. Chem Eur J. 2010;16:11558–11562.
[19] Chami F, Wilson MR, Oganesyan VS. Molecular dynamics and EPR spectroscopic studies of 8CB liquid crystal. Soft Matter. 2012;8:6823–6833.
[20] Meirovitch E, Igner D, Igner E, Mora G, Freed JH. Electron-spin relaxation and ordering in smectic and supercooled nematic liquid crystals. J Chem Phys. 1982;77:3915–3938.
[21] Wassmer KH, Ohmes E, Portugall M, Ringsdorf H, Kothe GJ. Molecular order and dynamics of liquid-crystal side-chain polymers: an electron spin resonance study employing rigid nitroxide spin probes. J Am Chem Soc. 1985;107:1511–1519.
[22] Xu D, Budil DE, Ober CK, Freed JH. Rotational diffusion and order parameters of a liquid crystalline polymer studied by ESR: molecular weigt dependence. J Phys Chem. 1996;100:15867–15872.
[23] Freed JH. Theory of slow tumbling ESR spectra for nitroxides. In: Berliner LJ, editor. Spin labeling: theory and applications. New York (NY): Plenum; 1976. p. 53–132.
[24] Schneider DJ, Freed JH, Calculating slow motional magnetic resonance spectra. A user's guide. In: Berliner LJ, Reuben J, editors. Biological magnetic resonance. New York (NY): Plenum; 1989. p. 1–75.

[25] Vorobiev AKh, Chumakova NA. Determination of orientation distribution function of anisotropic paramagnetic species by analysis of ESR spectra angular dependence. J Magn Reson. 2005;175: 146–157.
[26] Yankova TS, Bobrovsky AYu, Vorobiev AKh. Order parameters P2, P4 and P6 of aligned nematic liquid-crystalline polymer as determined by numerical simulation of electron paramagnetic resonance spectra. J Phys Chem B. 2012;116: 6010–6016.
[27] Chumakova NA, Vorobiev AKh. Simulation of rigid-limit and slow-motion EPR spectra for extraction of quantitative dynamic and orientational information. In: Kokorin AI, editor. Nitroxides – theory, experiment and applications [Internet]. Rijeka: InTech, 2012 [cited 2013 Apr 30]; p. 57–112. Available from: http://dx.doi.org/10.5772/48067, ISBN 978-953-51-0722-4.
[28] Vorobiev AKh, Yankova TS, Chumakova NA. Orientation distribution function and order parameters of oriented spin probe. Chem Phys. 2012;409: 61–73.
[29] Imazeki S, Mukoh A, Tanaka N, Kinoshita M. Unusual orientational behavior of anthraquinone dyes in nematic cyanophenylcyclohexane derivatives. Mol Cryst Liq Cryst. 1993;225:197–210.
[30] Vecchi I, Arcioni A, Bacchiocchi C, Tiberio G, Zanitaro P, Zannoni C. Expected and unexpected behavior of the orientational order and dynamics induced by azobenzene solutes in a nematic. J Phys Chem B. 2007;111:3355–3362.
[31] Chigrinov VG, Kozenkov VM, Kwok H-S. Photoalignment of liquid crystalline materials. West Sussex: Wiley; 2008.
[32] Fischer Th, Laesker L, Stumpe J, Kostromin SG. Photoinduced optical anisotropy in films of photochromic liquid crystalline polymers. J Photochem Photobiol A. 1994;80:453–459.
[33] Nakatsuji S, Fujino M, Hasegawa S, Akutsu H, Yamada J, Gurman VS, Vorobiev Akh. Azobenzene derivatives carrying a nitroxide radical. J Org Chem. 2007;72:2021–2029.
[34] Elyashevich G, Kozlov A, Moneva I. Study of polyethylene orientation in the course of porous structure formation. Polym Sci, Ser B. 1998;40:71–74.
[35] Bobrovsky A, Shibaev V, Elyashevitch G, Rosova E, Shimkin A, Shirinyan V, Bubnov A, Kaspar M, Hamplova V, Glogarova M. New photosensitive polymer composites based on oriented porous polyethylene filled with azobenzene-containing LC mixture: reversible photomodulation of dichroism and birefringence. Liq Cryst. 2008;35:533–539.
[36] Bobrovsky A, Shibaev V, Elyashevich G, Rosova E, Shimkin A, Shirinyan V, Cheng K-L. Photocromic composites based on porous stretched polyethylene filled by nematic liquid crystal mixtures. Polym Adv Technol. 2010;21(2):100–112.
[37] Dennis JE, Gay DM, Welsch RE. An adaptive nonlinear least-squares algorithm. ACM Trans Math Software. 1981;7:348–368.
[38] Zannoni C. Distribution functions and order parameters. In: Luckhurst GR, Gray GW, editors. The molecular physics of liquid crystals. New York (NY): Academic Press; 1979. p. 51–83.
[39] Blinov L. Structure and properties of liquid crystals. New York (NY): Springer Science Business Media B.V.; 2011.
[40] Budil DE, Lee S, Saxena S, Freed JH. Nonlinear-least-squares analysis of slow-motion EPR spectra in one and two dimensions using a modified Levenberg-Marquardt algorithm. J Magn Reson A. 1996;120:155–189.
[41] Cusati T, Granucci G, Persico M, Spighi G. Oscillator strength and polarization of the forbidden $n\rightarrow\pi^*$ band of trans-azobenzene: a computational study. J Chem Phys. 2008;128:194312-1–194312-9.
[42] Cusati T, Granucci G, Martínez-Nunez E, Martini F, Persico M, Vazquez S. Semiempirical hamiltonian for simulation of azobenzene photochemistry. J Phys Chem A. 2012;116:98–110.
[43] Weingart O, Lan Z, Koslowski A, Thiel W. Chiral pathways and periodic decay in cis-azobenzene photodynamics. J Phys Chem Lett. 2011;2: 1506–1509.